Supporting Information

Identification of Boronic Acid Derivatives as an Active Form of N-Alkylaminoferrocene-Based Anticancer Prodrugs and Their Radiolabeling with ^{18}F

Steffen Daum,[‡a] Johannes Toms,[‡b] Viktor Reshetnikov,[a] Hülya Gizem Özkan,[a] Frank Hampel,[a] Simone Maschauer,[b] Amir Hakimioun,[c] Frank Beierlein,[c] Leopold Sellner,[d] Michael Schmitt,[d] Olaf Prante,[b] Andriy Mokhir*[a]*

[a] Friedrich-Alexander University Erlangen-Nürnberg (FAU), Department of Chemistry and Pharmacy, Organic Chemistry Chair II, Nikolaus-Fiebiger-Str. 10, 91058 Erlangen, Germany

[b] Friedrich-Alexander University Erlangen-Nürnberg (FAU), Department of Nuclear Medicine, Molecular Imaging and Radiochemistry, Schwabachanlage 6, 91054 Erlangen, Germany

[c] Friedrich-Alexander University Erlangen-Nürnberg (FAU), Department of Chemistry and Pharmacy, Computer-Chemistry-Center and Interdisciplinary Center for Molecular Materials, Nägelsbachstr. 25, 91052 Erlangen, Germany

[d] *University Hospital Heidelberg, Department of Medicine V, 69120 Heidelberg, Germany*

Content:

Synthesis

Prodrug **9a** (the structure is given in Figures S1, 2) Starting material **1a** (300 mg, 601 μmol) was dissolved in acetone (5 mL). Diethanolamine (75.8 mg, 68.9 μL, 721 μmol) was added to the resulting solution, and the obtained mixture was stirred at 22 °C for 12 h. The precipitated product was isolated by centrifugation, washed with acetone (3 x 8 mL), re-crystallized from $CHCl_3$/ diethyl ether (Et_2O) solvent mixture and finally washed again with Et_2O. Orange crystals of product **9a** were obtained: 156.9 mg, 323 μmol, yield 54%. ^{1}H-NMR spectroscopy (400 MHz, DMSO-d_6): δ (ppm) = 7.46 (d, *J* = 7.6 Hz, 2H), 7.24 (d, *J* = 7.5 Hz, 2H), 6.89 (s, 1H), 5.12 (s, 2H), 4.51 (s, 2H), 4.46 (s, 2H), 4.21 (s, 5H), 4.06 (s, 2H), 3.94 – 3.82 (m, 2H),

3.82 – 3.73 (m, 2H), 3.34 (s, 1H), 3.16 – 3.00 (m, 2H), 2.90 – 2.72 (m, 2H). ^{13}C-NMR spectroscopy (101 MHz, DMSO-d_6): δ (ppm) 153.53, 145.91, 134.13, 132.68, 126.39, 100.05, 80.69, 74.63, 68.91, 67.60, 64.28, 62.96, 62.21, 50.67, 38.71. HR-ESI-MS (positive mode), *m/z*: calcd. 486.1408 for $C_{25}H_{27}BFeN_2O_4$ $[M\text{-}e^-]^+$, found 486.1420. Molecular structure of **9a** was confirmed by X-ray crystallography (Figure S1).

Prodrug **9b** (the structure is given in Figure 2) Compound **1b** (300 mg, 544 μmol) was dissolved in Et_2O (11 mL). Diethanolamine (68.7 mg, 62.4 μL, 653 μmol) in 2-propanol (0.4 mL) was added to the resulting solution, and the obtained mixture was stirred at 22 °C for 12 h. The precipitated product was isolated by centrifugation, washed with Et_2O (3 x 8 mL), re-crystallized from $CHCl_3$/Et_2O solvent mixture and finally washed again with Et_2O. Orange crystals of product **9b** were obtained: 156.9 mg, 323 μmol, yield 54%. ^{1}H-NMR spectroscopy (300 MHz, $CDCl_3$): δ (ppm) = 7.45 (d, J = 6.3 Hz, 2H), 7.38 – 7.04 (m, 7H), 5.16 (s, 1H), 5.04 (s, 2H), 4.91 (s, 2H), 4.34 (s, 2H), 4.07 (s, 5H), 3.93 (s, 2H), 3.91 – 3.71 (m, 4H), 3.11 – 2.83 (m, 2H), 2.63 – 2.40 (m, 2H). No high quality ^{13}C-NMR spectrum of this compound could be obtained due to its low solubility. High resolution electrospray mass spectrum (HR-ESI-MS, positive mode), *m/z*: calcd. 538.1721 for $C_{29}H_{31}BFeN_2O_4$ $[M\text{-}e^-]^+$, found 538.1725.

Prodrug **9c** (the structure is given in Figure 2) Prodrug **9c** was obtained similarly to **9b**, except that starting material **1c** was used in place of **1b** and the crude product was re-crystallized from acetone rather than the $CHCl_3$/Et_2O solvent mixture. Yield of **9b** is 66%. ^{1}H-NMR spectroscopy (400 MHz, $CDCl_3$): δ (ppm) = 7.61 – 7.38 (m, 2H), 7.36 – 7.22 (m, 2H), 7.22 – 7.05 (m, 4H), 6.11 (s, 1H), 5.10 (s, 2H), 4.90 (s, 2H), 4.35 (s, 2H), 4.09 (s, 5H), 3.94 (s, 2H), 3.84 – 3.58 (m, 4H), 3.44 (s, 2H), 3.08 – 2.80 (m, 2H), 2.54 – 2.38 (m, 2H), 2.38 – 2.21 (m, 4H), 1.69 – 1.49 (m, 4H), 1.49 – 1.33 (m, 2H). ^{13}C-NMR spectroscopy (101 MHz, $CDCl_3$): δ (ppm) = 155.55, 144.61, 138.69, 138.40, 135.47, 133.21, 128.77, 128.50, 127.83, 127.54,

125.45, 101.66, 77.69, 69.44, 68.50, 64.81, 63.72, 63.67, 63.02, 54.41, 51.59, 26.26, 24.52. HR-ESI-MS (positive mode), *m/z*: calcd. 636.2691 for $C_{35}H_{43}BFeN_3O_4$ $[M\text{-}e^-]^+$, found 636.2708.

Prodrug **11** (the structure is given in Figure 3) Starting material **1a** (50.0 mg, 100.2 µmol), 6-deoxy-6-fluoro-β-glucopyranosyl azide (**10**, 20.75 mg, 100.2 µmol) und CuI (3.82 mg, 20.0 µmol) were dissolved in tetrahydrofuran (THF, 1.5 mL), followed by the addition of triethylamine (TEA, 12.16 mg, 16.7 µL, 120.2 µmol). The reaction mixture was stirred at 22 °C for 12 h, then the solvent was removed *in vacuo* and the crude product was purified by column chromatography on silica gel using a solvent mixture CH_2Cl_2 / CH_3OH from 20/1 to 15/1 (v/v) as an eluent. Prodrug **11** was obtained as yellow solid. Yield: 50.0 mg, 70.8 µmol, 71%. Thin layer chromatography, R_f= 0.47 (silica, CH_2Cl_2 / CH_3OH 10/1, v/v). ^{1}H-NMR spectroscopy (400 MHz, acetone-d_6): δ (ppm) = 7.99 (s, 1H), 7.78 (d, *J* = 8.0 Hz, 2H), 7.46 (d, *J* = 8.0 Hz, 2H), 5.70 (d, *J* = 9.1 Hz, 1H), 5.63 (s, 1H), 5.25 (s, 2H), 5.06 (s, 2H), 4.86 – 4.48 (m, 7H), 4.15 (s, 5H), 4.03 (s, 1H), 4.00 (s, 2H), 3.92 – 3.79 (m, 1H), 3.70 (t, *J* = 8.9 Hz, 1H), 3.58 (t, *J* = 9.4 Hz, 1H), 1.35 (s, 12H); ^{13}C-NMR spectroscopy (75 MHz, acetone-d_6): δ (ppm) = 154.96 (s), 145.83 (s), 140.77 (s), 135.71 (s), 128.15 (s), 123.11 (s), 102.24 (s), 88.75 (s), 84.63 (s), 82.99 (d, J = 171.6 Hz), 78.70 (d, J = 18.0 Hz), 78.46 (s), 73.44 (s), 69.76 (s), 69.70 (s), 67.99 (s), 65.13 (s), 63.55 (s), 46.41 (s), 25.23 (s). HR-ESI-MS (positive mode), *m/z*: calcd. 706.2279 for $C_{33}H_{40}BFFeN_4O_8$ $[M\text{-}e^-]^+$, found 706.2282.

Prodrug **13** (the structure is given in Figure 3) Prodrug **13** was prepared analogously to **11** except that compound **12** was used as a starting material in place of **1a**. **13** was obtained as yellow solid. Yield: 59%. Thin layer chromatography, R_f= 0.15 (silica, CH_2Cl_2 / CH_3OH 20/1, v/v). ^{1}H-NMR spectroscopy (300 MHz, $CDCl_3$): δ (ppm) = 8.58 (s, 1H), 7.94 (d, *J* = 8.3 Hz, 2H), 7.74 (d, *J* = 7.2 Hz, 2H), 7.42 (d, *J* = 8.2 Hz, 4H), 5.76 (d, *J* = 9.2 Hz, 1H), 5.27 (s, 2H), 5.05 (s, 2H), 4.93 – 4.34 (m, 7H), 4.12 (s, 5H), 4.05 (d, *J* = 9.0 Hz, 1H), 4.01 – 3.96 (m, 2H),

3.88 (m, 1H), 3.72 (t, *J* = 8.9 Hz, 1H), 3.59 (t, *J* = 9.4 Hz, 1H), 1.33 (s, 12H); ^{13}C-NMR spectroscopy (101 MHz, acetone-d^6): δ (ppm) = 155.16 (s), 147.84 (s), 140.85 (s), 139.71 (s), 135.61 (s), 130.74 (s), 127.94 (s), 127.83 (s), 126.48 (s), 120.28 (s), 102.48 (s), 88.90 (s), 84.56 (s), 82.93 (d, J = 171.5 Hz), 78.63 (d, J = 17.8 Hz), 78.24 (s), 73.62 (s), 69.83 (s), 69.70 (d, J = 7.0 Hz), 67.94 (s), 65.14 (s), 63.24 (s), 53.97 (s), 25.19 (s). HR-ESI-MS (positive mode), *m/z*: calcd. 782.2588 for $C_{39}H_{44}BFFeN_4O_8$ $[M\text{-}e^-]^+$, found 782.2584.

Radiosynthesis of ^{18}F-fluoroglycosylated N-aminoferrocene-based prodrug [^{18}F]14

No-carrier-added [^{18}F]fluoride was produced through the ^{18}O(p,n)^{18}F reaction on a PETtrace 800 cyclotron using H_2[^{18}O]O as a target at the University Hospital Würzburg (Center of radiopharmacy, Würzburg, Germany). The synthesis of the labeling precursor 2,3,4-tri-*O*-acetyl-6-*O*-toluenesulfonyl-β-D-glucopyranosyl azide (**16**), nucleophilic ^{18}F-fluorination of **16** and deacetylation of the intermediate to obtain glucosyl azide [^{18}F]**10** in NaOH solution (60 mM, 270 µL) was performed as previously described.[1] Subsequently, the solution of [^{18}F]**10** was neutralized by the addition of phosphate buffer (pH 8, 0.5 M, 270 µL). A mixture of $Cu(OAc)_2$ (4 mM, 20 µL), tris[1-(3-hydroxypropyl)-1H-1,2,3-triazol-4-ylmethyl]amine (THPTA, 20 mM, 20 µL) and sodium ascorbate (0.1 M, 20 µL) was added to a solution of alkyne **12** (115 µg, 200 nmol, dissolved in 200 µL THF) and **13** (31 µg, 40 nmol, dissolved in 50 µL THF) and the resulting solution was added to the reaction vial containing [^{18}F]**2**. After the reaction time of 15 min at 60 °C, the radiochemical yield of [^{18}F]**14** was 85% as determined by analytical radio-HPLC from a sample withdrawn from the reaction vial. Radio-HPLC: t_R([^{18}F]**14**) = 16.69 min, t_R(**14**) = 16.54 min, t_R([^{18}F]**14**$^+$) = 10.76 min, t_R(**14**$^+$) = 10.61 min, t_R(**13**) = 23.10 min (Kromasil C8, 250 x 4.6 mm, 10-100% acetonitrile (0.1% trifluorocetic acid, TFA) in water (0.1% TFA) in a linear gradient over 30 min, 1.5 mL/min). All radioactive compounds were successfully identified by the retention time of the corresponding

nonradioactive references by HPLC. The time shift between the retention times of the radiolabeled compound and its nonradioactive reference compound corresponds to the distance between the UV detector and the radio-detector of the radio-HPLC system.

X-ray crystallography

Crystal structure of compound **9a** was deposited to the Cambridge Structural Database: CCDC 1838202. The crystals of **9a** showed surprisingly very poor diffraction at higher angles and more or less no diffraction at resolutions higher than 0.92 Angstrom for unknown reasons. The data set was acquired from the best crystal possible, which was achieved by several individual attempts for crystallization. Structure solution and refinement ended in a very good result of all other quality parameters without restrictions. Therefore, the minor lack in data at higher theta angles have no negative influence on the quality of the achieved structure.

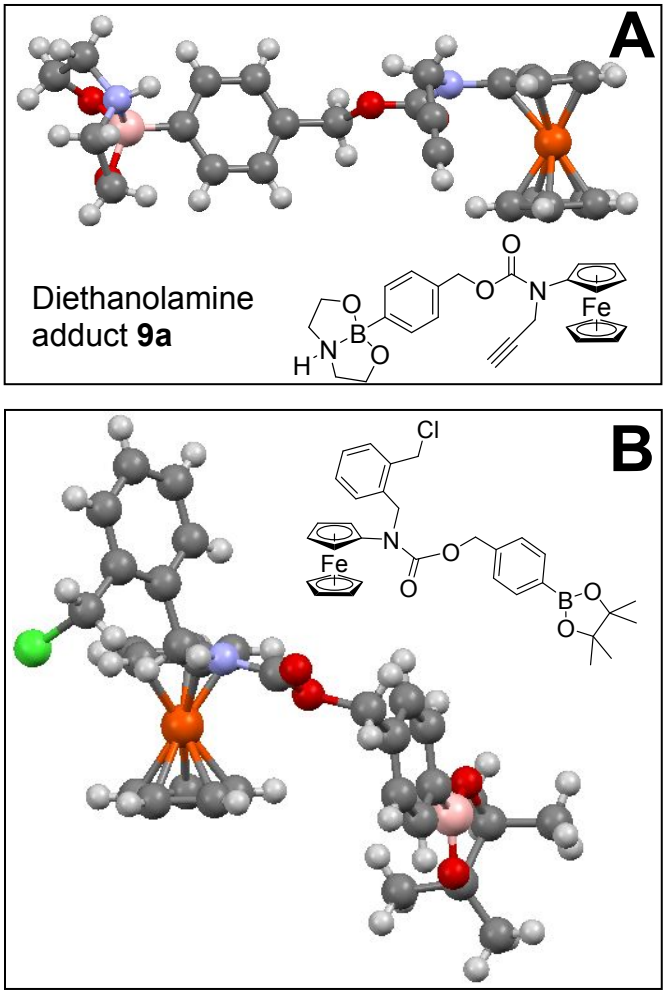

Figure S1. **A**: Molecular structure of **9a** determined by X-ray crystallography. **B**: Molecular structure of 4-[N-(3-chloromethylbenzyl)-N-ferrocenylaminocarbonyloxomethyl]phenyl-boronic acid pinacol ester reported elsewhere.[2]

Determination of n-octanol/water partition coefficients (logP values)

For the determination of logP values (octanol-water partition-coefficients) of prodrugs **1d, 11** and **13**, reversed phase - thin layer chromatography (RP-TLC, Macherey Nagel, Germany, ALUGRAM RP-18 W/UV_{254}, stationary layer thickness 0.150 mm) was applied. In particular, DMF/aqueous 3-(N-morpholino)propanesulfonic acid buffer (MOPS, 0.1 M, pH 7.4, 1/1, v/v) was applied as a mobile phase. A series of reference compounds with known logP values (benzyl alcohol (1.1), 8-hydroxyquinoline (1.9), benzophenone (3.18) and anthracene (4.5)) was chosen. Calibration plot of R_f versus logP was obtained to determine logP values of the

new prodrugs. The corresponding prodrugs (0.5 mM) were incubated at 37 °C for 18 hours in a mixture of DMF and phosphate-buffered saline (PBS: phosphate 10 mM, pH 7, NaCl 154 mM; DMF/PBS 1/1, v/v). TLC plates were then developed and the spots were visualized and marked with the help of UV-light at 254 nm. All experiments were done in triplicates.

Determination of hydrolytic stability of representative prodrugs

Stock solutions of prodrugs (**1a-d**, or **9c**, 2 mM) in DMSO were prepared. Then they were diluted 100-fold with (NEt_3H)(OAc) buffer (1.25 mM, pH 7). After that the probes (20 µL) of these solutions were injected to HPLC (column a Macherey–Nagel Nucleosil C18 250 x 4.6 mm) coupled to UV-visible detector (detection of absorbance at 260 nm) and quadrupole electrospray mass spectrometric detector (detection of positively charged ions in the *m/z* range of 100-1000) and eluted using gradients of CH_3CN (solvent B) in water (solvent A). Under these experimental conditions peaks corresponding to arylboronic acid pinacol esters (**1a-d**) as well as corresponding boronic acids (**8a-d**) appear broad and splitted probably due to formation of several adducts of the boron atom in these compounds with buffer components (Figure S2). They can include B-OAc, B-NEt_3, B-OH_2, B-OH etc. All these adducts give rise to single peaks in the MS-detection. For example, in the mixture obtained after hydrolysis of **1d** two peaks could be detected: *m/z* 671 corresponding to [**1d**+H^+]$^+$ and *m/z* 589 corresponding to [**1d**+H^+]$^+$. The adducts formation can be suppressed by replacing aqueous (NEt_3H)(OAc) buffer (1.25 mM) for the mixture of diluted phosphate buffer (0.1 mM) and CH_3CN (9/1, v/v) (see Figure 4, main text as an example). However, these conditions are less physiologically relevant due to the presence of the organic solvent. For example, we observed that addition of CH_3CN slows down the rate of boronic ester hydrolysis.

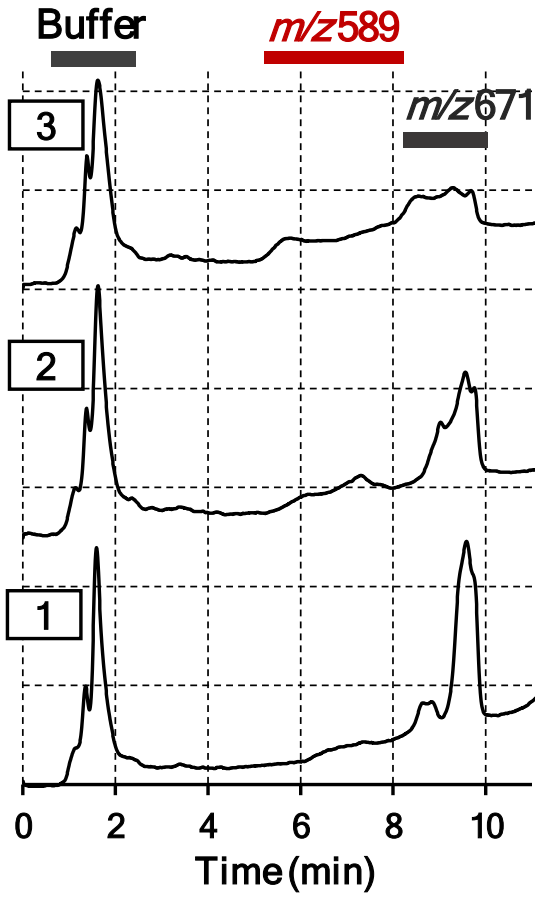

Figure S2. Study of hydrolytic stability of prodrug **1d** by using HPLC. The HPLC profile (absorbance at 260 nm *vs* time) of freshly prepared solution of prodrug **1d** (20 μM) in (NEt_3H)(OAc) buffer (1.25 mM, pH 7) containing DMSO (1 %, v/v) is labeled as 1. This solution was kept for 30 min (trace 2) and 60 min (trace 3) at 22 °C and analyzed under the same conditions by HPLC. To identify the products in HPLC fractions the quadrupole electrospray MS-detector (m/z 100-1000) was used. For each fraction mass spectra were acquired. Between 5.5 min and 8.2 min a signal at m/z 589 (indicated with a red thick bar) and between 8.4 min and 10 min a signal at m/z 671 (indicated with a black thick bar) were observed. Similar data were obtained for prodrugs **1a-c**. For **1a-d** half-lifetime was in aqueous neutral solution was found to be 42 $\pm$ 18 min.

Reference compound **8c**, which is an expected product of hydrolysis of both **1c** and **9c**, was prepared by controlled hydrolysis of **9c** in the presence of 0.1 M HCl. The formation of this

compound was confirmed by ^{1}H NMR spectroscopy (400 MHz, solvent $CDCl_3$; δ, ppm: 7.95 (2H), 7.22 (6H), 5.24 (2H), 4.92 (2H), 4.37 (2H), 4.09 (5H), 3.95 (2H), 3.56 (2H), 2.32 (4H), 1.56 (4H), 1.26 (3H)) as well as high resolution APPI-mass spectrometry (HR-APPI-MS, positive mode, *m/z*: calcd. 567.2112 for $C_{31}H_{35}BFeN_2O_4$ $[M+H^+]^+$, found 567.2121).

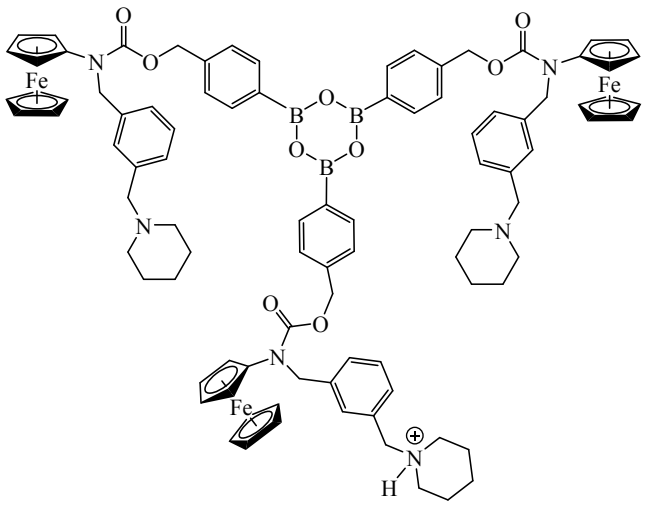

Chemical Formula: $C_{93}H_{100}B_3Fe_3N_6O_9^+$
Exact Mass: 1645,59

Figure S3. Chemical structure of a boroxine derivative, which can be formed by condensation of a representative boronic acid **8c**.

Monitoring generation of ROS in cell free settings

Generation of ROS was monitored using fluorescence spectroscopy as described earlier.[2] In particular, 2',7'-dichlorofluorescin diacetate (DCFH-DA, 4.9 mg) was dissolved in dimethylformamide (DMF, 100 μL) and mixed with aqueous NaOH (0.1 M, 900 μL). The resulting mixture was incubated for 30 min at 22 °C in the dark to obtain a stock solution of 2',7'-dichlorofluorescin (DCFH, 10 mM). Next a solution (1 mL) containing DCFH (10 μM), 3-(N-morpholino)propanesulfonic acid (MOPS) buffer (100 mM, pH 7.5), N,N,N',N'-ethylenediaminetetracetic acid (EDTA, 10 mM), glutathione (GSH, 5 mM), and H_2O_2 (10 mM) was prepared. Monitoring of the fluorescence (λ_{ex} = 501 nm, λ_{em} = 526-536 nm) of this solution was started. After 5 min, prodrugs (10 μL, 5 mM in DMSO, final concentration was 49.5 μM)

were added, and the fluorescence monitoring was continued until the fluorescence signal growth was stalled. The fluorescence intensity observed in this assay correlates with the amount of reactive ROS present in the mixture.

Table S1. Comparison of pairs of means (presented in rows in this table) by using Student's t-test (data from Table 1 of the main text of the article).

Prodrugs: PE-form / DEA-form[i]	ROS release (F/F_0)		Statistics:[ii]
	PE	DEA	df / p / ΔMean / CI
1a / **9a**	14.4 ± 1.2	15.9 ± 0.3	4 / 0.1036 / -1.5 / -3.483 <ΔMean< 0.483
1b / **9b**	8.2 ± 0.4	13.5 ± 0.6	4 / 0.0002 / -5.3 / -6.456 <ΔMean< -4.144
1c / **9c**	15.2 ± 1.0	14.3 ± 0.9	4 / 0.3110 / 0.9 / -1.257 <ΔMean< 3.057

[i] The DEA generate corresponding boronic acids upon their dissolution in aqueous neutral buffer as described in the main text of the paper.
[ii] df: degrees of freedom; p: two-tailed p value (two data sets were considered significantly different from each other for the probability $p < 0.05$); ΔMean: difference between a pair of mean values in the row; CI: 95 % confidence interval for ΔMean.

Table S2. Comparison of the mean ROS release factor $F/F_0 = 8.2 \pm 0.4$ determined for prodrug **1b** with the corresponding mean values obtained for a series of other prodrugs, which are indicated in the first column of this table, by using Student's t-test (data from Table 1 of the main text of the article).

Prodrug	ROS release (F/F_0)	Statistics: df / p / ΔMean / CI[i]
1a	14.4 ± 1.2	4 / 0.0011 / -6.200 / -8.228 <ΔMean< -4172
1c	15.2 ± 1.0	4 / 0.0004 / -7.000 / -8.726 <ΔMean< -5.274
9a	15.9 ± 0.3	4 / 0.0001 / -7.700 / -8.501 <ΔMean< -6.899
9c	14.3 ± 0.9	4 / 0.0004 / -6.100 / -7.679 <ΔMean< -4.521

[i] df: degrees of freedom; p: two-tailed p value (two data sets were considered significantly different from each other for the probability $p < 0.05$); ΔMean: difference between $F/F_0 = 8.2 \pm 0.4$ determined for prodrug **1b** and a corresponding value determined for prodrugs **1a**, **1c**, **9a**, **9c**; CI: 95 % confidence interval for ΔMean.

Monitoring of H_2O_2-induced activation of prodrug 13 using ESI mass spectrometry

A freshly prepared solution of prodrug **13** (5 µL, 4 mM in DMSO) was added to acetonitrile (50 µL). Next, water (200 µL) was added and pH of the resulting mixture was adjusted to pH 7 by using diluted aqueous solution of ammonia. Further, water was added to achieve the overall volume of the mixture of 498 µL. Finally, H_2O_2 (2 µL, 30% (w/w) in H_2O) was added and after 5 min incubation at 22 °C for 5 minutes, the mixture was diluted with acetonitrile (0.5 mL) and analyzed by high resolution ESI-TOF mass spectrometry.

Cells and cell culture

The human promyelocytic leukemia (HL-60) and human breast adenocarcinoma (MCF-7) cell lines were obtained from Sigma-Aldrich. The human prostate cancer cell line DU-145 was kindly provided by the laboratory of Prof. Dr. Helge Taubert (Clinic of Urology Friedrich-Alexander-University Hospital Erlangen). The human prostate cancer cell line PC-3 was obtained from the American Type Culture Collection (ATCC, CRL-1435™). The rat pancreatic tumor cell line AR42J was purchased from CLS Cell Lines Service GmbH (No 500478, Eppelheim, Germany). Burkitt lymphoma (BL-2) cells were obtained from Leibniz Institute DSMZ (German collection of microorganisms and cell cultures). Lung fibroblasts GM01379 were kindly provided by the laboratory of Prof. Dr. I. Ivanović-Burmazović (Department Chemistry and Pharmacy, Friedrich-Alexander-University Hospital Erlangen). The cells were cultured according to recommendations of DSMZ. In particular, HL-60, BL-2, DU-145 and PC-3 cells were grown in Roswell Park Memorial Institute (RPMI) 1640 medium (Biochrom GmbH, Germany) supplemented with either 20% (for BL-2) or 10% (for HL-60, DU-145, PC-3) fetal bovine serum (FBS, Biochrom GmbH, Germany), 1% L-glutamine, and 1% penicillin /streptomycin. MCF-7 and AR42J cells were grown in Dulbecco's modified eagle medium (DMEM, Biochrom GmbH, Germany) supplemented with 10% FBS, 1% L-glutamine, and 1%

penicillin/streptomycin. Suspension cells were grown to (0.5−1.5) × 10^6 cells/mL and diluted as required. Adherent cells were cultivated to 80−90% confluence.

Determination of the viability of non-adherent cancer cell lines (HL-60 and BL-2) The cells were centrifuged, the medium was removed, and the cells were washed two times with Dulbecco's phosphate buffered saline (DPBS) and re-suspended in RPMI 1640 medium containing 5% FBS, 1% L-glutamine, and 1% penicillin/ streptomycin. This suspension was spread in the wells of a 96-well microtiter plate (50.000 cells per well per 100 μL). Stock solutions of prodrugs of different concentrations (1 μL, solvent DMSO, final concentrations in wells were 1, 5, 10, 20, 50 μM) were added to the wells and incubated for 48 h at 37 °C under 5% CO_2. Four experiments were conducted for each concentration of the prodrug. Finally, 3-(4,5-dimethylthiazol-2-yl)-2,5-diphenyltetrazolium bromide (MTT, 20 μL of the solution prepared by dissolving MTT (5 mg) in phosphate buffered saline (PBS) buffer (1 mL)) was added to each well, incubated for 3 h, treated with sodium dodecyl sulfate (SDS) solution (90 μL, 10% solution in 0.01 M aqueous HCl), and incubated overnight. Afterward, the intensity of the absorbance at 590 nm was measured. MTT is converted in live cells to blue dye with the absorbance maximum λ_{max} at 590 nm. The absorbance at 690 nm was taken as a baseline value. The baseline corrected absorbance at 590 nm (A(590 nm) − A(690 nm)) was applied to calculate the relative number of viable cells. IC_{50} values were determined by fitting the experimental data expressing the number of viable cells (%, OY-axis) versus drug concentration (OX axis) with a sigmoidal curve using curve fitting software CurveExpert 1.4.

Table S3. Comparison of pairs of means (presented in rows in this table) by using Student's t-test (data from Table 1 of the main text of the article).

Prodrugs: PE-form / DEA-form[i]	IC_{50} (μM)[ii]		Statistics:[ii]
	PE	DEA	df / p / ΔMean / CI

1a / **9a**	25 ± 4	20 ± 1	10 / 0.0140 / 5 / 1.25 <ΔMean< 8.75
1b / **9b**	22 ± 2	13 ± 3	10 / 0.0001 / 9 / 5.72 <ΔMean< 12.28
1c / **9c**	3 ± 1	3 ± 1	10 / 1.000 / 0 / -1.29 <ΔMean< 1.29

[i] The DEA generate corresponding boronic acids upon their dissolution in aqueous neutral buffer as described in the main text of the paper.
[ii] df: degrees of freedom; p: two-tailed p value (two data sets were considered significantly different from each other for the probability $p < 0.05$); ΔMean: difference between a pair of mean values in the row; CI: 95 % confidence interval for ΔMean.

Determination of the viability of adherent cancer cell lines The medium was removed from the cultivated cells. The cells were washed two times with DPBS, trypsinated, and re-suspended either in DMEM supplemented with 5% FBS, 1% L-glutamine, and 1% penicillin/streptomycin (for MCF-7 and AR42J) or in RPMI 1640 medium supplemented with 10% FBS, 1% L-glutamine, and 1% penicillin /streptomycin (for DU-145 and PC-3). This suspension was spread in the wells of a 96-well microtiter plate (25.000 cells per well per 100 μL) and left standing at 37 °C in the chamber filled with CO_2 (5%) for 5 h. Stock solutions of prodrugs of different concentrations (1 μL, solvent DMSO, final concentrations in wells were 1, 5, 10, 20, 50 μM) were added to the wells and incubated for specific periods of time. Four experiments were conducted for each concentration of the prodrug. Finally, 3-(4,5-dimethylthiazol-2-yl)-2,5-diphenyltetrazolium bromide (MTT, 20 μL of the solution prepared by dissolving MTT (5 mg) in PBS buffer (1 mL)) was added to each well, incubated for 3 h, treated with sodium dodecyl sulfate (SDS) solution (90 μL, 10% solution in 0.01 M aqueous HCl), and incubated overnight. Afterward, the intensity of the absorbance at 590 nm was measured. MTT is converted in live cells to blue dye with the absorbance maximum λ_{max} at 590 nm. The absorbance at 690 nm was taken as a baseline value. The baseline corrected absorbance at 590 nm (A(590 nm) − A(690 nm)) was applied to calculate the relative number of viable cells. IC_{50} values were determined by fitting the experimental data expressing the number of viable cells (%, OY-axis) versus drug concentration (OXaxis) with a sigmoidal curve using curve fitting software CurveExpert 1.4.

Determination of the viability of fibroblasts GM01379 in the presence of prodrug **13** The DMEM medium was removed, and adherent GM01379 cells were washed two times with PBS, trypsinated, and re-suspended in DMEM medium containing 10% FBS, 1% L-glutamine, and 1% penicillin/streptomycin. This suspension was spread in the wells of a 96-well microtiter plate (10 000 cells per well per 100 μL) and left standing at 37 °C in the chamber filled with CO_2 (5%) overnight. Stock solutions of prodrug **13** of different concentrations (1 μL, solvent DMSO, final concentrations in wells were 1, 5, 10, 20, 50 μM) were added to the wells and incubated for specific periods of time. Three experiments were conducted for each concentration of the prodrug. Finally, 3-(4,5 dimethylthiazol-2-yl)-2,5-diphenyltetrazolium bromide (MTT, 20 μL of the solution prepared by dissolving MTT (5 mg) in PBS buffer (1 mL)) was added to each well, incubated for 3 h, treated with sodium dodecyl sulfate (SDS) solution (90 μL, 10% solution in 0.01 M aqueous HCl), and incubated overnight. Afterward, the intensity of the absorbance at 590 nm was measured. MTT is converted in live cells to blue dye with the absorbance maximum λ_{max} at 590 nm. The absorbance at 690 nm was taken as a baseline value. The baseline corrected absorbance at 590 nm (A(590 nm) − A(690 nm)) was applied to calculate the relative number of viable cells. IC_{50} values were determined by fitting the experimental data expressing the number of viable cells (%, OY-axis) versus drug concentration (OXaxis) with a sigmoidal curve using curve fitting software CurveExpert 1.4.

IC_{50} (prodrug **13**) = 48 ± 2 μM (n= 6).

Data for controls:

IC_{50} (prodrug **1d**) > 50 μM (n= 6).

IC_{50} (ferrocene) > 50 μM (n= 6).

Determination of viability of primary cancer (CLL) and normal (MNC) cells Clinical samples from chronic lymphocytic leukemia (CLL) patients (n=3) and peripheral blood mononuclear

cells (MNCs) from healthy donors (n=3) were collected at the University Hospital Heidelberg, Germany. Informed consent was obtained in accordance with the Declaration of Helsinki. Sample collection and analysis was approved by the ethics committee of the University of Heidelberg (S-254/2016). Blood was separated by a Ficoll gradient (GE Healthcarey), and cells were cryopreserved. Drug sensitivity screening was performed in 384-well format (Greiner Bio One) with 10 different prodrug concentrations (40, 20, 10, 5, 2.5, 1.25, 0.625, 0.313, 0.156, 0.078 µM) and $4x10^4$ cells per well. Cells were cultured in RPMI-1640 (Invitrogen) supplemented with penicillin/streptomycin (Invitrogen), L-glutamine (Invitrogen) and 10% pooled and heat inactivated AB-type human serum (Sigma-Aldrich). Cell viability was assessed by quantification of ATP (CellTiter Glo®, Promega) 48 hours after drug application. Luminescence was measured on a Tecan Infinite F200 Microplate Reader. Viability was calculated as % of solvent (DMSO) treated control (Figure S4).

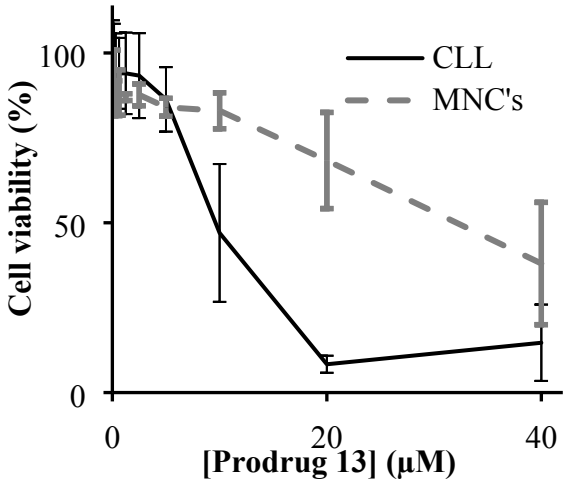

Figure S4. Effects of prodrug **13** on the viability of primary chronic lymphocytic leukemia (CLL) cells (black trace) and normal peripheral blood mononuclear cells (MNCs, grey trace). Detailed experimental conditions are given above.

Table S4. Comparison of pairs of means of IC_{50} values (presented in rows in this table) by using Student's t-test.

	IC_{50} (μM)[i]		Statistics:[ii]
	CLL cells	MNC's	df / p / ΔMean / CI
Prodrug **13**	9.3 ± 2.1	31 ± 12	4 / 0.0367 / 21.7 / 2.17 <ΔMean< 41.23

[i] IC_{50} is the concentration of prodrug **13**, at which half of the primary cells (CLL cells or MNC's) remains viable as determined by using CellTiter Glo® assay (Promega).
df: degrees of freedom; p: two-tailed p value (two data sets were considered significantly different from each other for the probability $p < 0.05$); ΔMean: difference between a pair of mean values in the row; CI: 95 % confidence interval for ΔMean.

In vitro stability of [^{18}F]**14 in human serum**

An aliquot of [^{18}F]**14** (80 μL) in a mixture of PBS (70%, 50 mM sodium ascorbate) and DMSO (30%) was added to human serum (400 μL) and incubated at 37 °C. Aliquots (80 μL) were taken at various time intervals (1−35 min) and quenched in 10% TFA/MeCN (1:1, 100 μL). The samples were centrifuged, and the supernatants were analyzed by radio-HPLC.

In vivo stability of [^{18}F]**14**

[^{18}F]**14** in PBS (70%, 50 mM sodium ascorbate) and DMSO (30%) (300 μL, 11-12 MBq) was injected in the tail vein of a Sprague-Dawley rat (Charles River). After 1, 3, 5, 10, 15 and 20 min blood samples were collected in heparin coated vials and centrifuged at 1500 g for 1 min. Afterwards, an aliquot from the supernatant was taken and quenched in the same volume of TFA (10%). These samples were centrifuged again (20000 g, 3 min) and the supernatants were analyzed by radio-HPLC.

Animal model

All animal experiments were performed in compliance with the protocols approved by the local Animal Protection Authorities (Regierung Mittelfranken, Germany, no. 54-2532.1-15/08). Female athymic nude mice (CD1-Foxn1/nu, homozygous) were obtained from Charles River

Laboratories (Germany) at 4 weeks of age and were kept under standard conditions (12 h light/dark) with food and water available ad libitum for at least 5 weeks. Viable cells were harvested, suspended in PBS/Matrigel (1:1, 100 µL) and were injected subcutaneously in the left (2×10^6 PC3 cells/mouse) and right (2.5×10^6 AR42J cells/mouse) back of the mice. Two weeks after inoculation, the mice, now weighing about 30 g and bearing tumors of 5-11 mm^3 in diameter, were used for small-animal PET studies.

PET imaging

PET scans and image analysis were performed using a small-animal PET scanner (Inveon, Siemens Medical Solutions). About 3−5 MBq [^{18}F]**14** were injected into each mouse (n = 3) either intravenously or subcutaneously under isoflurane anesthesia (4%). Animals were subjected to a dynamic 60 min-scan starting with tracer injection or a static PET scan at 45-60 min p.i. After iterative maximum a posteriori (MAP) image reconstruction of the decay and attenuation corrected images, regions of interest (ROIs) were drawn over the tumor and over muscle tissue as background region. The radioactivity concentration within the regions was obtained from the mean value within the multiple ROIs and then converted to %ID/g (percent injected dose per gram) relative to the injected dose.

Molecular modeling

Geometry optimizations were performed using B3LYP[3] hybrid density functional calculations with the 6-31G**[4-13] basis set and the D3 version of Grimme's dispersion correction with Becke-Johnson damping,[14] as implemented in Gaussian16.[15] The Polarizable Continuum Model (PCM) using the integral equation formalism variant (IEFPCM) was used to model solvent (water) influence (see reference[16] and the references cited therein). Frequency calculations of the optimized structures were performed to confirm stationary points (minima).

Two structures **11*** (hydrolyzed **11**) and **14** were constructed (Figures 3, S5). The sugar moiety was in chair conformation in all starting geometries. We focused on starting structures of intramolecular complexes with tetrahedral boron and bonds between boron and sugar oxygens O2', O3' and O4' (B-O distance approx. 1.45 Å). We optimized these compounds with deprotonated oxygens O2', O3' and O4' coordinated to boron (total charge -1). All calculations were repeated in vacuum to exclude possible problems with the implicit solvent model.

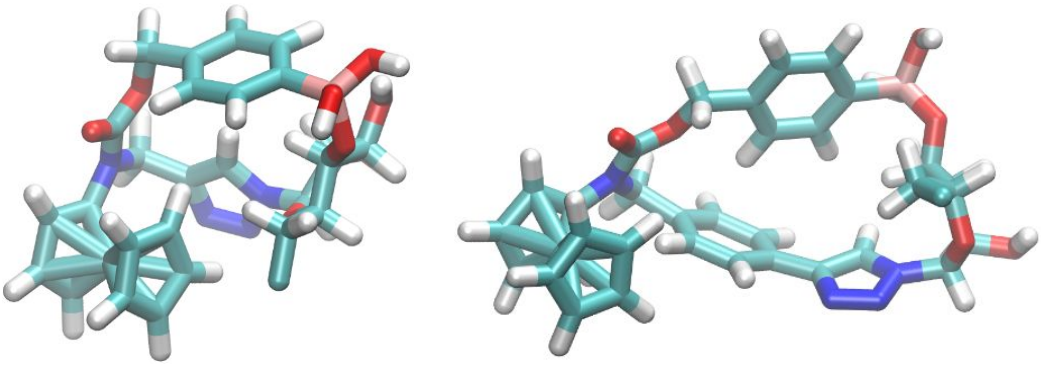

Figure S5. The optimized structures of **[11*/O4']**$^{-}$ (left) and **[14/O4']**$^{-}$ (right), which are the most stable forms of the adducts investigated. Figures were created using VMD.[17]

REFERENCES

(1) Maschauer, S.; Haubner, R.; Kuwert, T.; Prante, O. ^{18}F-Glyco-RGD Peptides for PET Imaging of Integrin Expression: Efficient Radiosynthesis by Click Chemistry and Modulation of Biodistribution by Glycosylation. *Mol. Pharm.* **2014**, *11(2)*, 505-515.

(2) Daum, S.; Chekhun, V.; Todor, I.; Lukianova, N.; Shvets, Y.; Sellner, L.; Putzker, K.; Lewis, J.; Zenz, T.; Graaf, I. et al. Improved synthesis of N-benzylaminoferrocene-based prodrugs and evaluation of their toxicity and antileukemic activity. *J. Med. Chem.* **2015**, *58(4)*, 2015-2024.

(3) Becke, A. D. Density-functional thermochemistry. III. The role of exact exchange. *J. Chem. Phys.* **1993,** *98*, 5648-5652.

(4) Ditchfield, R.; Hehre, W. J.; Pople, J. A. Self-Consistent Molecular-Orbital Methods. IX. An Extended Gaussian-Type Basis for Molecular-Orbital Studies of Organic Molecules. *J. Chem. Phys.* **1971,** *54*, 724-728.

(5) Hehre, W. J.; Ditchfield, R.; Pople, J. A. Self-Consistent Molecular Orbital Methods. XII. Further Extensions of Gaussian-Type Basis Sets for Use in Molecular Orbital Studies of Organic Molecules. *J. Chem. Phys.* **1972,** *56*, 2257-2261.

(6) Hariharan, P. C.; Pople, J. A. Influence of polarization functions on molecular-orbital hydrogenation energies. *Theor. Chem. Acc.* **1973,** *28*, 213-222.

(7) Hariharan, P. C.; Pople, J. A. Accuracy of AH equilibrium geometries by single determinant molecular-orbital theory. *Mol. Phys.* **1974,** *27*, 209-214.

(8) Gordon, M. S. The isomers of silacyclopropane. *Chem. Phys. Lett.* **1980,** *76*, 163-168.

(9) Francl, M. M.; Pietro, W. J.; Hehre, W. J.; Binkley, J. S.; DeFrees, D. J.; Pople, J. A.; Gordon, M. S. Self-Consistent Molecular Orbital Methods. 23. A polarization-type basis set for 2nd-row elements. *J. Chem. Phys.* **1982,** *77*, 3654-3665.

(10) Binning Jr., R. C.; Curtiss, L. A. Compact contracted basis-sets for 3rd-row atoms - GA-KR. *J. Comput. Chem.* **1990,** *11*, 1206-1216.

(11) Blaudeau, J.-P.; McGrath, M. P.; Curtiss, L. A.; Radom, L. Extension of Gaussian-2 (G2) theory to molecules containing third-row atoms K and Ca. *J. Chem. Phys.* **1997,** *107*, 5016-5021.

(12) Rassolov, V. A.; Pople, J. A.; Ratner, M. A.; Windus, T. L. 6-31G* basis set for atoms K through Zn. *J. Chem. Phys.* **1998,** *109*, 1223-1229.

(13) Rassolov, V. A.; Ratner, M. A.; Pople, J. A.; Redfern, P. C.; Curtiss, L. A. 6-31G* Basis Set for Third-Row Atoms. *J. Comput. Chem.* **2001,** *22*, 976-984.

(14) Grimme, S.; Ehrlich, S.; Goerigk, L. Effect of the damping function in dispersion corrected density functional theory. *J. Comput. Chem.* **2011,** *32*, 1456-1465.

(15) Frisch, M. J.; Trucks, G. W.; Schlegel, H. B.; Scuseria, G. E.; Robb, M. A.; Cheeseman, J. R.; Scalmani, G.; Barone, V.; Petersson, G. A.; Nakatsuji, H. et al. *Gaussian 16 Rev. B.01*, Wallingford, CT, 2016.

(16) Tomasi, J.; Mennucci, B.; Cammi, R. Quantum Mechanical Continuum Solvation Models. *Chem. Rev.* **2005,** *105*, 2999-3094.

(17) Humphrey, W.; Dalke, A.; Schulten, K. VMD - Visual Molecular Dynamics. *J. Molec. Graphics* **1996,** *14*, 33-38.